www.vbripress.com/aml, DOI: 10.5185/amlett.2016.6364 Published online by the VBRI Press in 2016

Structural and optical properties of bulk MoS_2 for 2D layer growth

Akhilesh Pandey[1]*, Shankar Dutta[1], Anand Kumar[1], R. Raman[1], Ashok K. Kapoor[1], R Muralidhran[2]

[1]*Solid State Physics Laboratory, DRDO, Lucknow Road, Timarpur, Delhi 110054, India*
[2]*Indian Institute of Science, Bengaluru, Karnataka 560012, India*

*Corresponding author. Tel: (+91) 11-23903761; E-mail: akhilesh.physics@gmail.com

Received: 14 December 2015, Revised: 10 February 2016 and Accepted: 03 June 2016

ABSTRACT

Molybdenum-di-sulfide (MoS_2) is being considered as an alternative 2-D material to graphene. Deposition of ultrathin MoS_2 layer from bulk MoS_2 sample is an important criterion in determining the viability of its application. This paper discusses about growth and characterization of bulk MoS_2 pellet from MoS_2 powder and exfoliation of MoS_2 layer from it. The MoS_2 pellets were sintered at different temperatures (500 - 850 °C) in nitrogen atmosphere. The sintered samples were found to be polycrystalline in nature with hexagonal flakes of 100 nm – 1.0 µm sizes. In addition to MoS_2 phase, surface of the bulk samples also has also some MoO_3 phase content, which was found to decrease with the increase in sintering temperature, confirmed by XRD. The optical absorption study showed MoS_2 absorptions around 1.82 eV, 2.01 eV due to spin orbit and direct band to band absorption from $\Gamma_{k\text{-}k}$ valley. The sintered MoS_2 samples were found to have characteristic Raman peaks of A_{1g} and E_{2g} with a separation of 26.5 cm^{-1}. Ultrathin MoS_2 layers, exfoliated from the sintered sample (850 °C), showed the reduced separation between Raman peaks A_{1g} and E_{2g} of 24.5 cm^{-1} few layer MoS_2. Copyright © 2016 VBRI Press.

Keywords: MoS_2; sintering; X-ray diffraction; Raman scattering.

Introduction

In recent years, layered materials in which atomic sheets (two-dimensional) are stacked together by weak Vander Waal forces are most comprehensively studied materials due to their unprecedented potential in electronic, optical, mechanical fields. It also has applications biological, chemical, thermal sensing [**1-10**]. After exploring the work on graphene by Novoselov and Geim in 2004 [**4**], it is the most well studied two-dimensional (2D) material [**1-3**, **5**]. Researchers are also exploring other novel 2D materials, like nitrides (e.g., h-BN), di-chalcogenides (e.g., MoS_2), topological insulators (e.g., Bi_2Se_3 or Bi_2Te_3) and even oxides, which could compliment graphene in different applications [**1-2**, **6-13**].

Layered transition metal di–chalcogenides (LTMDC), like molybdenum-di-sulfide (MoS_2), have been studied in the past due to its potential applications as solid catalysts [**14**], lubricants [**15-16**], hydrogen storage material [**17**], and photo-voltaic [**18-20**] and so on. Bulk form of MoS_2 has an indirect band gap (1.23 eV) [**21**]. In 2010, Splendiani *et al.* [**6**] and Mak *et al.* [**7, 12**] independently discovered an indirect-to-direct band-gap transition in MoS_2 when varying the thickness from bulk to monolayer (1.8 eV). This non- trivial band-gap makes monolayer MoS_2 a better choice for electronic and photonic devices than graphene (zero band-gap). In 2011, a single layer MoS_2 transistor was demonstrated with a high on/off ratio (~10^8), high current density and a room-temperature mobility of more than 200 cm^2/ Vs [**8**]. In 2012, few research groups reported about valley selective optical excitation and luminescence in monolayer MoS_2 [**12-13, 18-19, 21-23**]. Optical absorption tri-layer MoS_2 combined with PbS quantum dot have been studied recently by Mukherjee *et al.* [**24**]. Mechanical properties of single-layer MoS_2 were presented by Gomez *et al.* [**25**] and Bertolazzi *et al.* [**26**] respectively.

Deposition of high quality large area MoS_2 ultrathin films is one of the most crucial factors in determining the feasibility of its application. Many different techniques are being employed to realize nano-sized single or few layer MoS_2 films. Techniques like chemical vapor deposition (CVD) [**27-29**], sputtering [**19,30**], pulsed laser deposition (PLD) [**31**], spin-coating [**20**], evaporation [**32**], heating of Mo with sulfur environment [**33**], to achieve MoS_2 films have been used extensively to grow MoS_2 films. Loh *et al.* [**34**] has grown the MoS_2 thin film by PLD at 500 °C on catalytic metal foils and studied the 2D layer behavior. Researchers have also used mono layer MoS_2 in hetero-junction solar cells and field effect transistor based devices [**35, 36**]. Many researchers used mechanical exfoliation ("scotch-tape method") to get large area, high-quality, atomically flat MoS_2 layers [**25, 32**]. Among them, sputtering, PLD, mechanical exfoliation requires bulk sample to deposit MoS_2 thin films. Moreover, studies on bulk MoS_2 can provide complementary information for understanding mono-layers and their interaction with environments and substrates.

In last few years some efforts are being made to know properties of bulk MoS_2 for understanding MoS_2 mono-layers and their interaction [**6, 10**]. Kumar *et al.* [**21**] reported transient absorption microscopy study of charge carrier dynamics in bulk MoS_2 crystals at room

temperature. Paradisanos *et al.* [**37**] discussed about the effect of femto second laser irradiation on bulk and single-layer MoS_2 on silicon-oxide substrate. Flux method growth of bulk MoS_2 single crystals and its application as saturable absorber was discussed by Zhang *et al.* [**38**]. Laskar *et al.* [**27**] presented effect of annealing temperature (500 - 1100 °C) in grain growth of MoS_2 thin films deposited by sulfurization of e-beam evaporated molybdenum.

In this work, bulk MoS_2 samples are grown by sintering MoS_2 pellet which is made from MoS_2 powder. The effects of sintering temperatures on MoS_2 grain growth have been studied and reported. Phase analysis of the MoS_2 samples was studied by x-ray diffraction (XRD) and Raman Spectroscopy techniques. The optical properties of MoS_2 using optical absorption are studied. From the bulk samples, mechanically exfoliated MoS_2 thin layer is characterized by Scanning Electron Microscopy (SEM) and Raman spectroscopy is also reported. In addition to the source of mechanical exfoliation, the bulk MoS_2 samples can be used in future as target material for deposition of ultrathin MoS_2 layers by sputtering or PLD techniques.

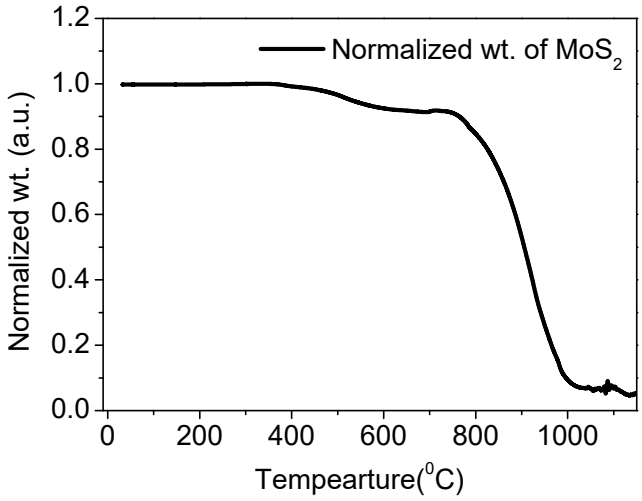

Fig. 1. TGA graph of MoS_2 powder normalized weight verses temperature.

Experimental

To prepare bulk MoS_2 pellets, 99 % pure MoS_2 powder was used (Make: Sigma Aldrich, USA). A number of MoS_2 pellets of 10 mm diameter were prepared by hydraulic press technique. The MoS_2 pellets were then sintered in a three-zone horizontal furnace at different temperature starting from 500 – 850 °C for 4 hours under nitrogen environment. The N_2 gas flow-rate was kept at 2000 sccm during the whole process.

Thermo gravimetric analysis (TGA) (Model: METTLER TOLEDO) of MoS_2 powder was done under nitrogen atmosphere starting from 50 – 1150 °C to find out the dissociation temperature for MoS_2 grain growth. Phase analysis of the bulk MoS_2 samples were done by x-ray diffraction technique in θ-2θ scan mode using Cu K_α radiation (Model: PANalytical X-Pert Pro MRD HRXRD system). Surface morphologies of the sintered samples were studied by Field-Emission Scanning Electron Microscopy (FE-SEM) (SUPRA-55). Raman spectroscopy experiments were done at room temperature by Horiba Jobin Yuvan LABRAM HR Evolution Confocal Micro-Raman spectrometer system using visible excitation frequency doubled NdYAG laser at 532 nm with cooled UV enhanced CCD detector, in the back scattering geometry. Reflectance measurements were done in the specular reflection mode by Cary series Agilent UV-visible Spectrophotometer system for optical absorption related study. A very thin layer of MoS_2 was mechanically exfoliated from the sintered sample (850 °C) by scotch tape method. The exfoliated layer was then studied by SEM and Raman spectroscopy.

Results and discussion

Fig. 1 shows the normalized weight verses temperature for MoS_2 powder on sample holder in N_2 ambient condition. In N_2 environment, a slight weight loss was seen around 350 °C, which is due to adsorbed moisture in MoS_2 powder but the decomposition of MoS_2 started around 800 °C**.** Thus from the TGA results, the sintering temperature of MoS_2 pellets was decided around 500 – 850 °C range in pure N_2 environment and maximum sintering temperature of MoS_2 pellet was fixed at 850 °C.

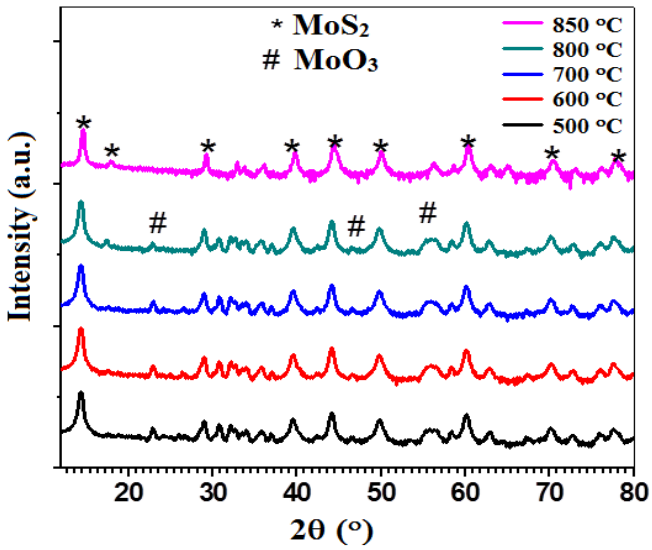

Fig.2. X-ray diffraction patterns of MoS_2 samples sintered at 500 – 850 °C in nitrogen for 4 hours.

Before each sintering process, the MoS_2 pellets were first placed inside the furnace at room temperature and nitrogen gas was flushed in the tube for 30 minutes to minimize the oxygen contamination and formation of MoO_3 phase. This step is very essential, to avoid MoO_3 growth on the surface of the sintered MoS_2 pellets. After the sintering processes, crystal structure of the sintered MoS_2 pellet was studied by X-ray diffraction (XRD) technique. **Fig. 2** shows the XRD patterns of the sintered MoS_2 pellets. The sintered pellets were found to be polycrystalline in nature and the peaks were well-matched with JCPDS (77-1716) MoS_2 file. The sintered samples showed prominent XRD peaks at 14.6°, 29.3°, 39.8°, 44.35°, 50.05°, 60.35°, 70.3° and 77.85°

corresponding to the (002), (004), (103), (104), (105), (008), (200) and (0010) crystallographic planes respectively. The XRD data also indicates presence of MoO_3 phase at the surface of the sintered pellets. The XRD peaks at 23.3°, 49° and 58.3° were corresponding to the (110), (200) and (112) planes of orthorhombic crystal structure of MoO_3 (data matched with JCPDS (75-0912) file). As molybdenum oxidizes at very low temperature (~ 70 °C), formation of MoO_3 phase was observed along with the MoS_2 phase in the sintering pellets. Here, the source of oxygen seems to be due to the absorbed moisture and air during pellet formation.

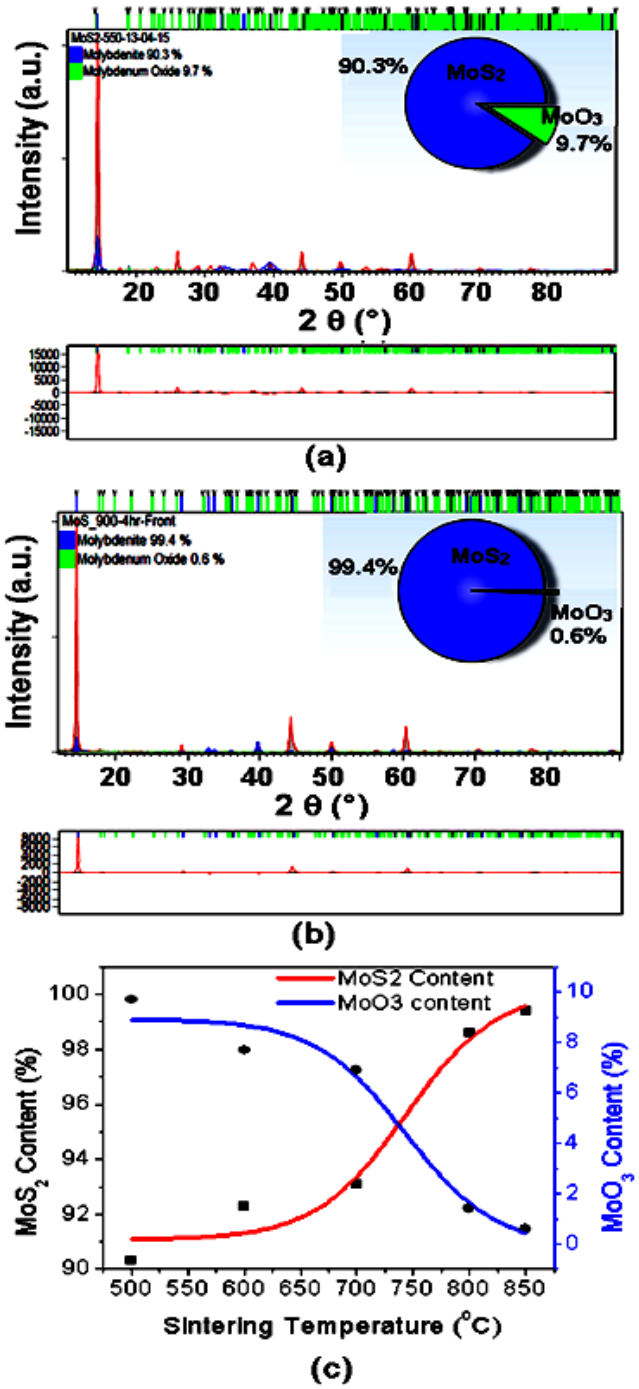

Fig. 3. Rietveld analyses of the MoS_2 and MoO_3 phases (%) in the pellets sintered at (a) 500 °C, (b) 850 °C, and (c) content of MoS_2 and MoO_3 with sintered temperature.

Average crystallite sizes (MoS_2 grains) were calculated by Debye Scherer method. The average crystallite size was found to be increased from 30 nm to 47 nm with the increase in sintering temperature from 500 °C to 850 °C. To know the phase contents of the MoS_2 and MoO_3 phases in the sintered pellets, XRD data were analyzed by Rietveld refinement method by using PANalytical high score plus software in multiphase mode. Rietveld analyses of the MoS_2 and MoO_3 phases (%) in the pellets sintered at 500 and 850 °C are shown in **Fig. 3**(**a**) and (**b**) respectively. The sintered pellet at 500 °C shows the MoO_3 content of 9.7 % and MoS_2 content of 90.3 % as shown in **Fig. 3**(**a**). The MoS_2 content starts to increase and the MoO_3 content starts decreasing with the increasing sintered temperature. After 800 °C sintered temperature the MoS_2 content saturated around ~99 %. At 850 °C, the sintered pellet showed the MoS_2 content ~ 99.4 % while MoO_3 content was around 0.6 %. The contents of MoS_2 and MoO_3 phases with sintering temperatures are shown in **Fig. 3**(**c**). It is known that MoO_3 starts sublimating around 600 °C and sublimate completely around 800 °C [**39**]. Thus the content of MoO_3 from the MoS_2 pellet starts decreasing with the increase in sintering temperature.

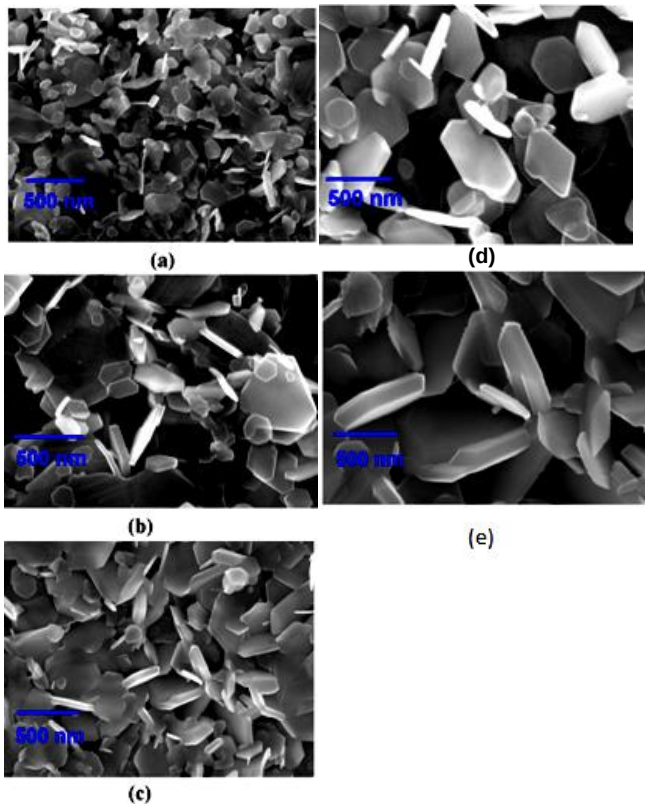

Fig. 4. FE-SEM micrographs of MoS_2 pellets sintered at (a) 500°C, (b) 600°C, (c) 700°C, (d) 800°C and (e) 850°C.

Surface morphologies of the sintered MoS_2 pellets are shown in **Fig. 4**. From the SEM images, one can see the growth of MoS_2 flakes. The MoS_2 pellets sintered at 500 °C and 600 °C showed (**Fig. 4**(**a**) and (**b**)) two different types of grains: a number of smaller hexagonal grains (100 – 200 nm sizes) and few bigger grains (0.5 – 1 µm sizes). The smaller hexagonal grains are of MoS_2 while the bigger

grains correspond to the MoO_3. As the sintering temperature increases to 700 °C, the grains of MoO_3 almost disappeared and uniform grains of MoS_2 are observed as depicted in **Fig. 4**(**c**). With further increase in sintering temperatures, size of the MoS_2 grains also increases as shown in **Fig. 4**(**d**) and (**e**). Size of the MoS_2 flakes are found to increase from 200 – 250 nm to 0.8 – 1.0 µm with the increase in sintering temperature from 700 °C to 850 °C.

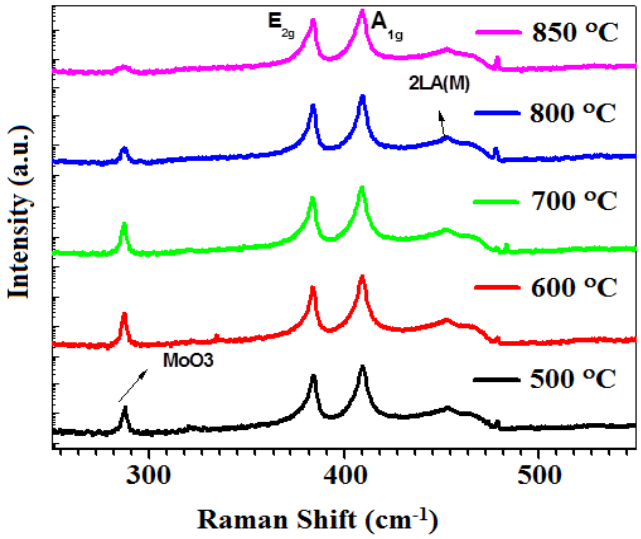

Fig. 5. Raman spectra of sintered MoS_2 samples from at 500 – 850 °C.

Hexagonal MoS_2 belongs to P63/mmc (194) group and contains two molecular units with total six atoms in a unit cell [**40**]. There are 12 allowed lattice vibration modes i.e. $A_{1g}+2A_{2u}+2B_{1u}+B_{1u}+E_{1g}+2E_{1u}+2E_{2g}+E_{2u}$ [**32**]. Since E symmetry is doubly degenerate symmetry, therefore total 18 modes exit. Out of 18 phonon modes 3 are acoustic and 15 are optical phonon modes. Among them, A_{1g}, E_{1g}, E^2_{1g}, E^2_{2g} modes are Raman active [**41**]. The A_{1g} (408 cm^{-1}) corresponds to in plane vibrations of S atoms and E_{2g} (382 cm^{-1}) corresponds the out of plane vibration of Mo and S atoms.

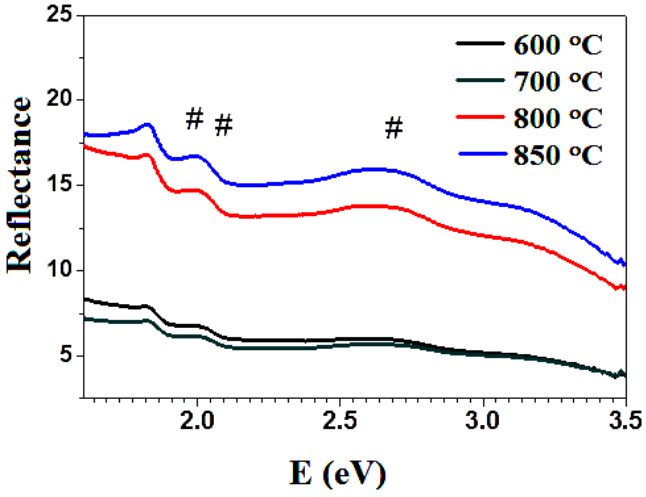

Fig. 6. Optical reflectance of sintered MoS_2 samples.

Fig. 5 shows the Raman spectra of the sintered MoS_2 pellets. Measurement was carried out using 100 X objectives and with very low power (1-2 mW) to avoid sample heating. All the sintered samples exhibited the A_{1g} and E_{2g} Raman peaks of MoS_2 at 382 cm^{-1} and 408.5 cm^{-1} respectively as shown in **Fig. 5**. Difference of these two peaks is observed around 26.5 cm^{-1}. The intensities of the Raman peaks were found to be increasing with the increase of sintering temperature. Maximum intensity of the A_{1g} and E_{2g} Raman peaks was observed MoS_2 sample sintered at 850 °C. It shows the improvement of MoS_2 crystalline quality with the sintering temperature. A weaker peak around 453 cm^{-1} was also observed and this peak is due to a secondary phonon mode 2 LA (M) of MoS_2 [**41-42**]. In addition to the A_{1g}, E_{2g} and 2 LA (M) Raman peaks, another peak is observed at 288 cm^{-1} in sintered pellets. This peak corresponds to MoO_3 Raman peak [**43**]. However, the Raman peak of MoO_3 was found to be decreases with the increase in sintered temperature. The MoS_2 sample sintered at 850 °C showed minimal MoO_3 content.

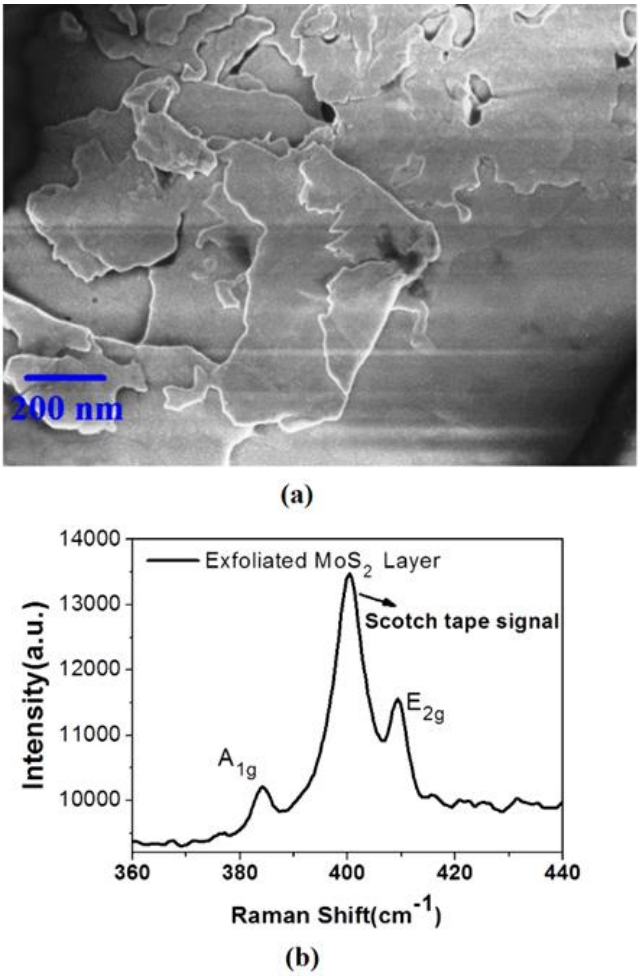

Fig. 7. Exfoliated few layer MoS_2 (a) FE-SEM micrograph and (b) Raman spectra.

To study the optical absorption in MoS_2 samples is shown in **Fig. 6**, UV-visible spectrophotometer experiments were done in the reflection mode because MoS_2 pellets

were thick (~1 mm) and backside of the pellets was very rough. The semi-infinite geometry results the reflectance features primarily due to the dielectric function from the one side of the reflecting surface. A reflectance spectrum of MoS_2 sintered pellets at different temperature from 600 – 850 °C are recorded from visible wavelength range from 400 – 900 nm and are shown in **Fig. 6**. It can be seen that absorption increases with the increase in sintering temperature. Absorption at 1.82 eV was due to spin orbit splitting of valance band [**44-45**]. Direct band-edge absorption $\Gamma_{k\text{-}k}$ ($Eg_{k\text{-}k}$) [**45**] was also observed at 2.01 eV. One strong reflectance peak was also observed at 2.63 eV which may be due to higher order symmetric transition, where the valance and conduction bands are parallel with respect to each other.

Mechanical exfoliation of a very thin layer of MoS_2 was done from bulk MoS_2 sample sintered at 850 °C by scotch tape method. FESEM micrograph and Raman spectra of mechanically exfoliated MoS_2 layered thin film are shown in **Fig. 7**(**a**) and (**b**) respectively. The FESEM image clearly shows the exfoliated layer is few layer MoS_2. The Raman spectra of the exfoliated MoS_2 layer showed a decrease in the separation between A_{1g} and E_{2g} peaks (24.5 cm^{-1}) compared to that of the bulk MoS_2 samples (26.5 cm^{-1}). The decrease in separation between the Raman peaks is consistent with previous report [**32**]. The exfoliated MoS_2 layer also showed a strong broad hump around 395 cm^{-1}, which is attributed to scotch tape used for the exfoliation. The exfoliated MoS_2 layer can be used for different electronic devices and sensors in future.

Conclusion

In this paper, growth of simple and cost effective method of bulk MoS_2 sample by sintering of MoS_2 powder is discussed. The MoS_2 samples are sintered in a three-zone horizontal furnace under nitrogen atmosphere for 4 hours. The sintering temperature range (500 – 850 °C) was decided by thermo-gravimetric analysis. From the XRD analysis, the sintered samples were found to be polycrystalline in nature. At lower sintering temperatures (500–600 °C), presence of MoO_3 phase was also observed at the bulk MoS_2 surface, but with increase in temperature (850 °C) the MoO_3 phase content was found to be minimized (< 1%). Growth of hexagonal MoS_2 flakes during the sintering process was also reported in this study. Size of the MoS_2 flakes were found to increase from 100 – 200 nm to 0.8 – 1.0 µm with the increase in sintering temperature from 500 °C to 850 °C respectively. Optical properties of the sintered MoS_2 samples were studied using Raman spectroscopy and UV-visible spectroscopy. The absorption is found to be increased with the sintering temperature. Split off orbital (SOV) absorptions was observed around 1.82 eV and direct band edge absorption from K valley was also observed at 2.01 eV. The low temperature sintered samples showed presence of Raman peaks corresponding to both MoS_2 and MoO_3 phases. At higher temperature (850 °C) the MoO_3 Raman peak is diminished. The sintered MoS_2 samples were found to have characteristic Raman peaks of A_{1g} and E_{2g} with a separation of 26.5 cm^{-1}. Therefore, it can be concluded 850 °C is the best optimized sintered temperature for bulk MoS_2 sample. The exfoliated MoS_2 layers from the MoS_2 sample showed the reduced separation between Raman peaks A_{1g} and E_{2g} of 24.5 cm^{-1}. Apart from the exfoliation technique, the bulk samples can also be utilized as target material for deposition of ultrathin MoS_2 layer by PLD or sputtering techniques. Thin film MoS_2 layer can be widely used in optoelectronics, transistors and gas sensors.

Acknowledgements

The authors acknowledge Director SSPL for his continuous support and for the permission to publish this work. Authors also want to acknowledge to Mr. Sandeep Dalal for XRD experiments. Help from other colleagues are also acknowledged.

References

1. Butler, S. Z.; Holler, S. M.; Cao, L.; Cui, Y.; Gupta, J. A.; Gutiérrez, H. R.; Heinz, T. F.; Hong, S. S.; Huang, J.; Ismach, A. F.; Halperin, E. J.; Kuno, M.; Plashnitsa, V. V.; Robinson, R. D.; Ruoff, R. S.; Salahuddin, S.; Shan, J.; Shi, L.; Spencer, M.G.; Terrones, M.; Windl, W.; Goldbergere, J. E.; *ACS Nano*., **2013**, *7*, 2898. **DOI:** 10.1021/nn400280c
2. Rogers, J. A.; Someya, T.; Huang, Y.; *Science*, **2010**, *327*, 1603. **DOI**: 10.1126/science.1182383
3. Geim, A. K.; *Science*, **2009**, *324*, 1530. **DOI**: 10.1126/science.1158877
4. Novoselov, K.S.; Geim, A.K.; Morozov, S.V.; Jiang, D.; Zhang, Y.; Dubonos, S.V.; Grigorieva, I.V.; Firsov, A. A.; *Science*, **2004**, *306*, 666. **DOI**: 10.1126/science.1102896
5. Zang, J.; Cao, C.; Feng, Y.; Liu, J.; Zhao, X.; *Scientific Reports*, **2014**, *4*, 6492. **DOI**: 10.1038/srep0692
6. Splendiani, A.; Sun, L.; Zhang, Y.; Li, T.; Kim, J.; Chim, C. Y.; Galli, G.; Wang, F.; *ACS Nano Lett.*, **2010**, *10*, 1271. **DOI:** 10.1021/nl903868w
7. Mak, K.F.; Lee, C.; Hone, J.; Shan, J.; Heinz, T. F.; *Phys. Rev. Lett.*, **2010**, *105*, 136805. **DOI**: 10.1103/PhysRevLett.105.136805
8. Radisavljevic, B.; Radenovic, A.; Brivio, J.; Giacometti, V.; Kis, A.; *Nat. Nanotech.*, **2011**, *6*, 147. **DOI**: 10.1038/nnano.2010.279
9. Tyagi,J.; Kakkar,R.; *Adv. Mat. Lett.*, **2013**, *4*, 721. **DOI**: 10.5185/amlett.2013.3438
10. Chaturvedi, A.; Tiwari, A,; Tiwari, A,; *Adv. Mat. Lett.*, **2013**, *4*, 656. **DOI**: 10.5185/amlett.2013.4469
11. Zeng, H.; Dai, J.; Yao, W.; Xiao, D.; Cui, X.; *Nat. Nanotech.*, **2012**, *7*, 490. **DOI**: 10.1038/nnano.2012.95
12. Mak, K. F.; He, K.; Shan, J.; Heinz, T. F.; *Nat. Nanotech.*, **2012**, *7*, 494. **DOI**: 10.1038/nnano.2012.96
13. Xiao, D.; Liu, G. B.; Feng, W.; Xu, X.; Yao, W.; *Phys. Rev. Lett*., **2012**, *108*, 196802. **DOI**: 10.1103/PhysRevLett.108
14. Hu, K. H.; Huand, X.G.; Sun, X.J.; *Appl. Surf. Sci.*, **2010**, *256*, 2517. **DOI**: 10.1016/j.apsusc.2009.10.098
15. Kim, Y.; Huang, J. L.; Lieber, C. M.; *Appl. Phys. Lett*., **1991**, *59*, 3404. **DOI**: 10.1063/1.105689
16. Fleischauer, P. D.; *Thin Solid Films*, **1987**, *154*, 309. **DOI**: 10.1016/0040-6090(87)90375-0
17. Chen, Z.; Cummins, D.; Reinecke, B. N.; Clark, E.; Sunkara, M. K.; Jaramillo, T. F.; *ACS Nano Lett.*, **2011**, *11*, 4168. **DOI:** 10.1021/nl2020476
18. Fortin, E.; Sears, W.; *J. Phys. Chem. Sol.*, **1982**, *43*, 881. **DOI**: 10.1016/0022-3697(82)90037-3

19. Tao, J.; Chai, J.; Guan, L.; Pan, J.; Wang, S.; *Appl. Phys. Lett.*, **2015**, *106*, 081602.
DOI: 10.1063/1.4913662
20. Shanmugam, M.; Bansal, T.; Durcan, C. A.; Yu, B.; *Appl. Phys. Lett.*, **2012**, *100*, 153901.
DOI: 10.1063/1.3703602
21. Kumar, N.; He, J.; He D.; Wang, Y.; Zhao, H.; *J. Appl. Phys.*, **2013**, *113*, 133702.
DOI: 10.1063/1.4799110.
22. Cao, T.; Wang, G.; Han, W.; Ye H.; Zhu, C.; Shi, J.; Niu, Q.; Tan, P.; Wang, E.; Liu, B.; Feng, J.; *Nat. Commun.*, **2012**, *3*, 887.
DOI: 10.1038/ncomms1882
23. Sallen, G.; Bouet, L.; Marie, X.; Wang, G.; Zhu, C. R.; Han, W. P.; Lu, Y.; Tan, P. H.; Amand, T.; Liu, B. L.; Urbaszek, B.; *Phys. Rev. B*, **2012**, *86*, 081301.
DOI: 10.1103/PhysRevB.86.081301
24. Mukherjee, B.; Guchhait, A.; Chan, Y.; Simsek, E.; *Adv. Mater. Lett*., **2015**, *6*, 936.
DOI: 10.5185/amlett.2015.6094
25. Gomez, A.C.; Poot, M.; Steele, G. A.; VanderZant, H. S. J.; Agrait, N.; Bollinger, G.R.; *Adv. Mater.*, **2012**, *24*, 772.
DOI: 10.1002/adma.201103965
26. Bertolazzi, S.; Brivio, J.; Andras, K.; *ACS Nano*, **2011**, *5*, 9703.
DOI: 10.1021/nn203879f
27. Laskar, M. R.; Ma, L.; Kannappan, S.; Park, P.S.; Krishnamoorthy, S.; Nath, D.N.; Lu, W.; Wu, Y.; Rajan, S.; *Appl. Phys. Lett.*, **2013**, *102*, 252108.
DOI: 10.1063/1.4811410
28. Ling, X.; Lee, Y.H.; Lin, Y.; Fang, W.; Yu, L.; Dresselhaus, M.S.; Kong, J.; *ACS Nano Lett.*, **2014**, *14*, 464.
DOI: 10.1021/nl4033704
29. Sigiro, M.; Nasruddin, M.N.; *Optik*, **2015**, *126*, 666.
DOI: 10.1016/j.ijleo.2014.07.140
30. Vierneusel, B.; Schneider, T.; Tremmel, S.; Wartzack, S.; Gradt, T.; *Surf. Coat. Tech.*, **2013**, *235*, 97.
DOI: 10.1016/j.surfcoat.2013.07.019
31. Late, D.J.; Shaikh, P.A.; Khare, R.; Kashid, R.V.; Chaudhary, M.; More, M.A.; Ogale, S.B.; *ACS Appl. Mater. Interfaces*, **2014**, *6*, 15881.
DOI: 10.1021/am503464h
32. Balendhran, S.; Ou, J.Z.; Bhaskaran, M.; Sriram, S.; Ippolito, S.; Vasic, Z.; Kats, E. ; Bhargava, S.; Zhuiykov, S.; Kalantar-zadeh, K.; *Nanoscale*, **2012**, *4*, 461.
DOI: 10.1039/C1NR10803D
33. Gaur, A.P.S.; Sahoo, S.; Ahmadi, M.; Guinel, M.J.F.; Gupta, S.K.; Pandey, R.; Dey, S. K.; and Katiyar, R.S.; *J. Phys. Chem. C*, **2013**, *117*, 26262.
DOI: 10.1021/jp407377g
34. Loh, T. A. J.; Chua, D. H. C.; *ACS Appl. Mater. Interfaces*, **2014**, *6*, 15966.
DOI: 10.1021/am503719b
35. Guo,Y,; Wei, X.; Shu, J.; Liu, B.; Yin, J.; Guan, C.; Han, Y.; Gao, S.; Chen, Q.; *Appl. Phys. Lett.*, **2015**, *106*, 103109.
DOI: 10.1063/1.4914968
36. Tsai, M.; Su, S. H.; Chang, J. K.; Tsai, D. S.; Chen, C. H.; Wu, C. I.; Li, L.J.; Chen, L.J.; He, J.H.; *ACS Nano*, **2014**, *8*, 8317.
DOI: 10.1021/nn502776h
37. Paradisanos; Kymakis, E.; Fotakis, C.; Kioseoglou, G.; Stratakis, E.; *Appl. Phys. Lett.*, **2014**, *105*, 041108.
DOI: 10.1063/1.4891679
38. Zhang, X.; Lou, F.; Li, C.; Zhang, X.; Jia, N.; Yu, T.; He, J.; Zhang, B.; Xia, H.; Wang, S.; Tao, X.; *Cryst. Eng. Comm.*, **2015**, *17*, 4026.
DOI: 10.1039/C5CE00484E
39. Kulyuk, L.; Charron, L.; Fortin, E.; *Phys. Rev. B*, **2003**, *68*, 075314.
DOI: 10.1103/PhysRevB.68.075314
40. Wieting,T.; Verble, J.; *Phys. Rev. B*, **1971**, *3*, 4286.
DOI: 10.1103/PhysRevB.3.4286
41. Verble J.; Wieting T.; *Phys. Rev. Lett.*, **1970**, *25*, 362.
DOI: 10.1103/PhysRevLett.25.362
42. Zhang, X.; Han, W.; Wu, J.; Milana, S.; Lu, Y.; Li, Q.; Ferrari, A.; Tan, P.; *Phys. Rev. B*, **2013**, *87*, 115413.
DOI: 10.1103/PhysRevB.87.115413
43. Chen, Y.; Lu, C.; Xu, L.; Ma, Y.; Hou, W.; Zhu, J. J.; *Cryst. Eng. Comm*, **2010**, *12*, 3740.
DOI: 10.1039/c000744g
44. Hu, B.; *Semi. Sci. Technol.*, **2015**, *30*, 055013.
DOI: 10.1088/0268-1242/30/5/055013
45. Visic, B.; Dominko, R.; Gunde, M. K.; Hauptman, N.; Skapin, S. D.; Remskar, M.; *Nanoscale Res. Lett.*, **2011**, *6*, 593.
DOI: 10.1186/1556-276X-6-593